ACS APPLIED MATERIALS & INTERFACES

www.acsami.org
Research Article

Enhancing Thermo-Mechanical Properties of Liquid Crystal Elastomers through Chain Entanglements

Devyansh Agrawal, Gaoweiang Dong, and Shengqiang Cai*

Cite This: ACS Appl. Mater. Interfaces 2025, 17, 30094−30102

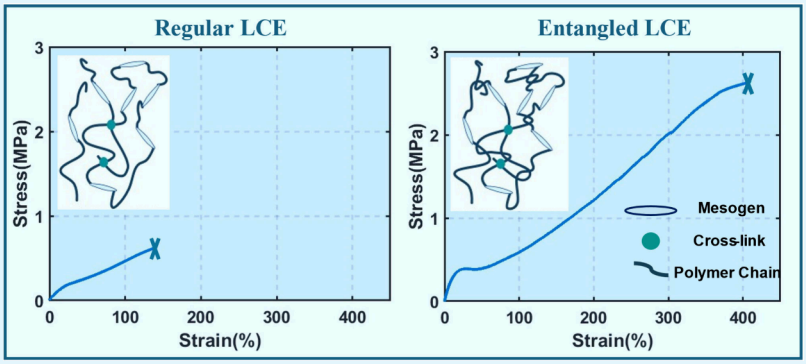

ABSTRACT: In this study, we present an approach to enhance the thermo-mechanical performance of liquid crystal elastomers (LCEs) by inducing chain entanglements through mechanical kneading. This process creates a network of highly entangled polymer chains, significantly improving the mechanical properties of LCEs, over a wide range of strain rates and temperatures. Mechanical kneading also improves the actuation performance, resulting in higher actuation stresses, greater contraction, and increased tolerance to self-rupture at elevated temperatures. Chain entanglements can also serve as a crucial enabler for the fabrication of monodomain LCEs. Using entanglements as the initial cross-linking step provides sufficient elasticity to LCEs, enabling the synthesis of aligned LCEs. This work demonstrates the benefits of chain entanglements, offering a pathway for the design and fabrication of high-performance LCE-based actuators for advanced applications.

KEYWORDS: *Liquid Crystal Elastomer (LCE), Chain Entanglements, Mechanical Kneading, Polymer Processing, Soft Actuators, Thermo-Mechanical Performance*

1. INTRODUCTION

Liquid crystal elastomers (LCEs) represent a fascinating class of materials that merge the elasticity of conventional elastomers with the anisotropic properties of liquid crystals, resulting in remarkable features like reversible actuation and soft elasticity.[1,2] Their stimuli-responsive actuation is driven by phase transitions between the ordered nematic and disordered isotropic states, which enable LCEs to generate substantial actuation forces and large deformations. This makes them highly valuable for various applications such as sensors and actuators.[3−9]

LCEs have also emerged as excellent damping materials, making them promising candidates for applications involving vibration suppression and impact protection.[10,11] Additionally, LCEs have shown potential as advanced adhesives, utilizing their soft elasticity nature, enhanced dissipative properties, and tunable anisotropy for pressure-sensitive adhesive applications.[7,12] Further improvement of the mechanical properties of LCEs to enhance their versatility is always desirable and could facilitate their broader adoption for practical applications.

In this study, we propose to improve thermo-mechanical performance of LCEs through introducing polymer chain entanglements. While previous studies have investigated the influence of cross-linking density on the thermo-mechanical properties of LCEs, both in theory and through experiments,[13−15] a critical factor—polymer chain entanglements—has remained largely unexplored. Entanglements are a fundamental feature in most polymer networks, inherently present, and essential to understanding their behavior. Entanglements in polymer networks are known to significantly influence the mechanical properties of elastomers, such as strength, toughness, and fatigue resistance.[16] However, the effect of these entanglements on LCEs, which also exhibit

Received: February 26, 2025
Revised: April 28, 2025
Accepted: April 28, 2025
Published: May 7, 2025

https://doi.org/10.1021/acsami.5c04077
ACS Appl. Mater. Interfaces 2025, 17, 30094−30102

distinct thermal actuation behavior, remains to be investigated. Molecular dynamic simulations have indicated that increasing the entanglement density in these polymers could enhance their mechanical performance.[17,18]

Drawing inspiration from previous studies that reported a method for processing highly elastic and tough hydrogels and dry elastomers,[19,20] this study presents a technique for inducing entanglements in LCEs through mechanical kneading. This process involves repeated folding and compression of the material to increase the entanglement density of polymer chains. In cross-linked polymer networks with sparse entanglements, energy dissipation is confined to individual polymer chains between cross-links when a chain breaks. In contrast, networks with dense entanglements distribute tension across longer chains during stretching, allowing for greater energy dissipation upon fracture. As a result, entanglements enhance toughness while preserving elasticity.

Fully cross-linked LCEs typically result in Polydomain LCEs, but many applications require Monodomain LCEs. Various methods have been adopted in the past to synthesize Monodomain LCEs.[2,21−24] The alignment of mesogens required for Monodomain LCEs can be achieved through either a one-step or two-step process. One-step processes, such as external field and surface alignment methods, are highly sensitive to the intensity of the applied fields, often resulting in limitations such as inconsistent alignment and a high defect density.[23] In contrast, the two-step process involves initially polymerizing the mesogens into a loosely cross-linked polymer network, followed by mechanical stretching to align the mesogens and then fixing them into the Monodomain state through further polymerization. Often different cross-linking polymerization reactions are utilized for the two steps: fast and slow cross-linking; thermal and free-radical based photo-cross-linking; or dynamic covalent bonds.[1,2] More recently, 3D printing of LCEs has also been explored, achieving mesogen alignment via the shearing of viscous LCE ink.[25,26] In this study, we demonstrate that entanglements can act as the first cross-linking step, enabling the synthesis of Monodomain LCEs and thereby broadening the range of cross-linking reactions available for Monodomain LCE fabrication.

We believe that gaining an understanding of whether such entanglements in LCEs could improve mechanical properties such as strength, stiffness, and extensibility, particularly at high temperatures, while also enhancing actuation performance, could open new avenues for the development of better material actuators with a wider range of applications.

2. MATERIALS AND METHODS

Materials. 4-(6-(Acryloyloxy)hexyloxy) benzoate (C6BAPE, Chemfish, 97%), 2,2′-(ethylenedioxy) diethanethiol (EDDET, Sigma−Aldrich, 95%), (2-hydroxyethoxy)-2-methylpropiophenone (HHMP, Sigma−Aldrich, 98%), dipropylamine (DPA, Sigma−Aldrich, 98%), and the solvent dichloromethane (CH_2Cl_2) were used as received without further purification. For the above chemicals, we maintained a stoichiometry of $2n_{C6BAPE}$:$2n_{EDDET}$ = 50:49 for the fabrication of LCEs. All of the chemical structures can be found in Figure S1.

Synthesis and Fabrication of Entangled Polydomain LCE Films. To prepare the LCE mixture, we first added the monomer C6BAPE (10.0000 g, 21.3 mmol) to dichloromethane (10.0000 mL). Next, we sequentially added the chain extender EDDET (3.3866 g, 18.58 mmol) and catalyst DPA (0.0324 g, 0.32 mmol), along with dichloromethane (30.0000 mL). We then stirred the solution on a magnetic stirring plate at 300 rpm for 24 h. Lastly, we added the photoinitiator HHMP (0.0772 g, 0.34 mmol) and stirred for another 5 min.

We then concentrated the mixture through forced air drying by introducing a controlled airflow of 6−8 L/min for 45 min, resulting in a viscous ink-like solution. Next, we evaporated the LCE ink at 85 °C for 8 h to remove excess solvent, forming an LCE dough.

We placed the LCE dough between two aluminum plates (McMaster-Carr 1655T8) with two sheets of parchment paper and a 0.25 mm-thick Teflon spacer positioned on one side of the top sheet and then compressed it using a hydraulic press (model 4386, CARVER) at a pressure of 4 metric tons for 10 min at room temperature. The dough gradually flattened into a thin sheet, matching the Teflon spacer thickness.

We then folded the sheet four times, two times along the longitudinal axis and two times along the vertical axis, on a cold plate before compressing it again, completing one kneading cycle. After seven additional kneading cycles, we cross-linked the resulting sheet under ultraviolet light (365 nm wavelength) for 60 min, yielding an Entangled Polydomain LCE sheet. In contrast, omitting the kneading process and cross-linking the sheet under ultraviolet light yields a Regular Polydomain LCE sheet. The Entangled LCE appears more opaque compared to the Regular LCE (Figure S2).

Fabrication of Entangled Monodomain LCE Films. After eight cycles of kneading, we placed the Entangled LCE sheet under ultraviolet light (365 nm wavelength) for 10 min. Next, we positioned it on a substrate layer of commercially available 3M VHB tape. We then uniaxially stretch the substrate, bonded with the LCE layer, until the LCE reaches twice its original length. Thereafter, we cross-link the stretched LCE under ultraviolet light (365 nm wavelength) for 30 min. Finally, we carefully debond the LCE film from the substrate, yielding an Entangled Monodomain LCE sample.

Uniaxial Tensile Tests of Polydomain LCE Samples. We conducted mechanical tests of Entangled and Regular LCE using RSA-G2 (TA Instruments) in uniaxial tensile mode, with rectangular samples (height: 10 mm, width: 3 mm, thickness: ∼0.25 mm), across a temperature range between 40 and 150 °C for the LCEs. The uniaxial tension tests for the LCE at 25 °C and at different strain rates were conducted using an Instron tensile tester, with a 1 KN load cell, with the same sample dimensions. The strain rate applied for all of the tests at different temperatures was 1%/s.

Actuation Stress and Strain Measurements of (Pre-stretched) Polydomain LCE Samples. To measure the actuation stress, we used the RSA-G2 instrument (TA Instruments). We first applied different levels of prestretch to the LCE sample (height: 10 mm, width: 3 mm, thickness: ∼0.25 mm), by running a uniaxial tension test module with a strain rate of 1%/s. We then held the sample in the prestretched state for a certain relaxation time determined by a stress relaxation experiment. Next, we performed a temperature sweep module from 25 to 120 °C, with a 10 °C/min heating ramp rate, and measured the actuation force. The actuation stress was equal to the force divided by the initial cross-sectional area.

To measure the actuation strain, the LCE sample (height: 20 mm, width: 5 mm, thickness: ∼0.25 mm) with external load in the form of hanging weights was placed in a temperature-controlled glass chamber. After hanging the weights, we waited for 5 min at room temperature for the sample to stabilize and then increased the temperature rapidly to observe the contraction of the sample. We characterized the length and the actuation strain of LCE samples at each weight by analyzing the images taken with a digital camera (Canon 80D), using MathWorks (MATLAB, image processing toolbox).

Uniaxial Tensile Tests and Actuation Characterization of Entangled Monodomain LCE Samples. We characterized the actuation stress, actuation strain, and self-rupture temperature of Entangled Monodomain LCE samples (height: 20 mm, width: 0.5 mm, thickness: ∼0.15 mm) using the RSA-G2. We encapsulated the LCE samples and parts of the analyzer in a temperature-controlled chamber. For blocked stress measurements, we mechanically clamped the LCE samples on both sides and measured the actuation forces

https://doi.org/10.1021/acsami.5c04077
ACS Appl. Mater. Interfaces 2025, 17, 30094−30102

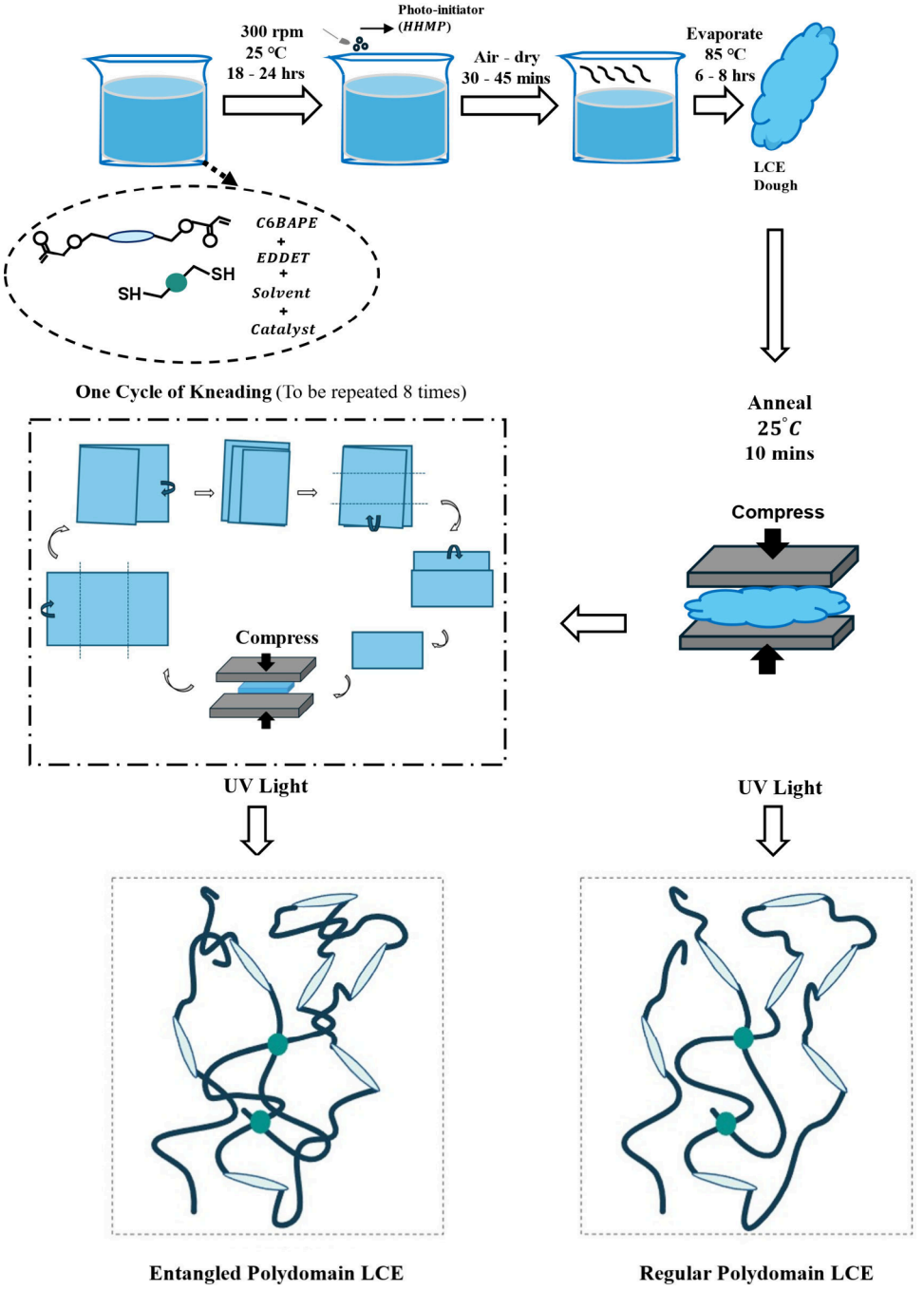

Figure 1. Fabrication process of Entangled LCE. Schematic illustrating the synthesis of LCE dough, followed by mechanical kneading of the LCE dough to create a highly entangled LCE. The kneading process induces a higher density of entanglements compared to the Regular LCE.

while gradually increasing the temperature at a ramp rate of 5 °C/min.

To measure the free actuation strain, we clamped the LCE samples at the top, while leaving the bottom free. As the temperature increased, the LCE samples began to contract. We then adjusted the bottom clamp location and recorded the distance between the two clamps at each temperature step.

We also performed mechanical tests on Entangled Monodomain LCEs at different temperatures using an RSA-G2 (TA Instruments) in uniaxial tensile mode, with rectangular samples (height: 20 mm, width: 0.5 mm, thickness: ∼0.15 mm). We used the freestanding length at 25 °C as the reference to calculate the strain.

Differential Scanning Calorimetry (DSC) Measurement of LCE Samples. We conducted DSC measurements using a Discovery DSC 250 instrument (TA Instruments) in a nitrogen atmosphere. We sealed the 5 mg LCE samples in aluminum pans and set the heating and cooling scanning rate to 5 °C/min within a temperature range between −10 and 100 °C.

Thermogravimetric Analysis (TGA) of LCE Samples. We conducted TGA measurements using a Discovery SDT 650 instrument (TA Instruments) under a nitrogen atmosphere. We set the heating rate to 10 °C/min within a temperature range between 20 and 800 °C.

Dynamic Mechanical Analysis (DMA) of LCE Samples. We conducted DMA analysis using RSA-G2 (TA Instruments) in tensile mode, with rectangular samples (height: 10 mm, width: 3 mm, thickness: ∼0.25 mm). The samples were first preloaded to 1% strain and then cycled at 0.1% strain at 1 Hz and heated from −60 to 100 °C at a rate of 5 °C/min. The glass transition (T_g) was defined as the maximum of the tangent delta (tan δ) curve.

https://doi.org/10.1021/acsami.5c04077
ACS Appl. Mater. Interfaces 2025, 17, 30094−30102

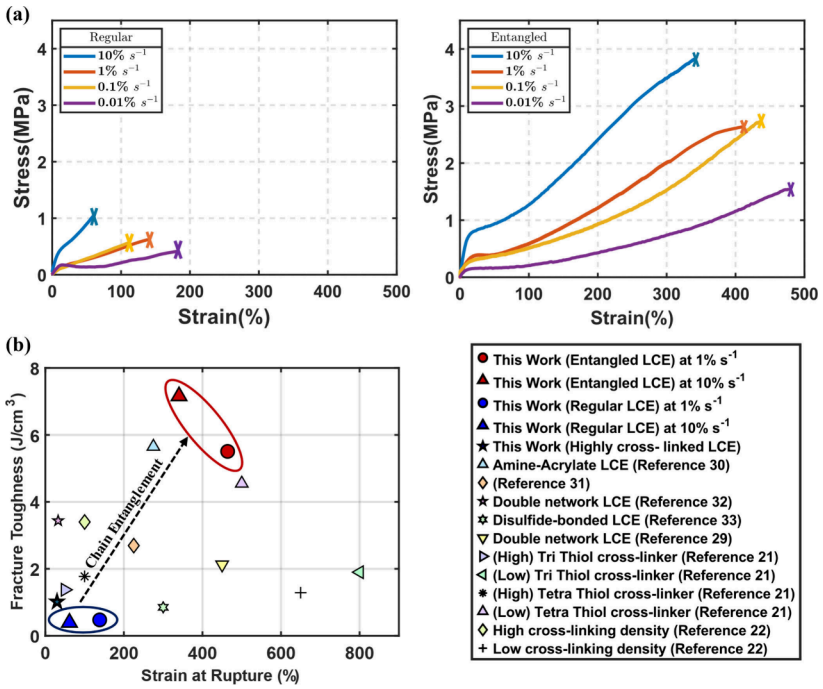

Figure 2. Mechanical properties of Entangled LCE. (a) Comparison of stress−strain curves between Regular and Entangled LCEs, at different strain rates. (b) Comparison of fracture toughness and strain at rupture of Entangled Polydomain LCEs with various other Polydomain LCEs in the literature.

3. RESULTS AND DISCUSSION

3.1. Processing and Fabrication of Entangled LCE Films. We synthesize a highly viscous LCE solution by first introducing a steady air stream into the dilute LCE mixture, containing mesogen, solvent, spacer, and catalyst to accelerate solvent evaporation. Next, we remove the remaining solvent by heating the solution at a high temperature, resulting in the formation of a highly conformable, dough-like liquid crystal polymer melt containing negligible residual solvent, which is confirmed by TGA tests shown in Figure S3. We then compress the dough between two aluminum plates for 10 min at room temperature, forming a rectangular sheet. To increase the entanglement of liquid crystal polymers, we knead the dough by folding the sheet four times, creating a stacked sheet, followed by compression again. This process is repeated for eight cycles, yielding a highly entangled LCE sheet. Finally, the Entangled LCE undergoes UV curing for 60 min to complete the photopolymerization-induced cross-linking of the polymer network (Figure 1).

This repeated process of folding and kneading the polymer sheet induces numerous entanglements within the polymer network, causing the chains to interweave, which restricts their ability to slide freely past one another when they are stretched. The resulting LCE exhibits a fabric-like topology, characterized by a cross-linked network with dense entanglements. In contrast, omitting the kneading process results in a Regular LCE with a cross-linked net-like topology and sparse entanglements.[19,27] In highly cross-linked and sparsely entangled polymers, when stretched, tension is distributed across short chain segments and transferred to other chains through cross-links. When a single covalent bond breaks, only the energy stored in these short chains dissipates, leading to low toughness. In contrast, in densely entangled polymers, tension is spread over many longer polymer chains. This network of entanglements enables the polymer to dissipate elastic energy across many chains over long lengths when a single covalent bond breaks, resulting in higher toughness.[18,19] The entanglements in these polymers also ensure a more uniform distribution of tension both within and between chains, effectively acting as slip-links to enhance stiffness.[28]

3.2. Improvement in Mechanical Properties of LCEs through Chain Entanglements. It is well-known that, at temperatures below T_{ni}, when LCEs are subject to a load, an initial increase in stress is followed by a distinctive stress plateau due to soft elasticity. Within this plateau, the mesogens gradually rotate to align with the direction of the applied load. As temperature increases, the length of this plateau decreases progressively and eventually disappears at temperatures above T_{ni}.[25] This soft elasticity stress plateau, resulting from mesogen rotation, is a characteristic feature of LCEs.[1,2] However, we did not observe an apparent stress plateau for both Entangled and Regular LCEs tested at room temperature, at a strain rate of 1%/s, as evidenced in Figure 2. Prompted by this observation, we tested both LCEs at different strain rates and found a more pronounced stress plateau for them at lower strain rates. At higher strain rates, the viscous response of LCEs becomes more pronounced, thereby to some extent masking the soft elasticity plateau. In contrast, at lower strain rates, the elastic behavior of LCE becomes more apparent, allowing the mesogens to gradually rearrange and align in the direction of applied strain, contributing to a more evident stress plateau in the stress−strain curve. Across the tested strain rates of 0.01%/s, 0.1%/s, 1%/s, and 10%/s, Entangled LCEs were observed to be almost four times stronger and nearly three times more stretchable compared to Regular LCEs.

Though systematic optimization of the mechanical behaviors of LCEs is not the main objective of this work, we found that our Entangled LCE demonstrated higher fracture toughness compared to various Polydomain LCEs in the literature[21,22,29−33] (Figure 2b). We observed that entanglements

https://doi.org/10.1021/acsami.5c04077
ACS Appl. Mater. Interfaces 2025, 17, 30094−30102

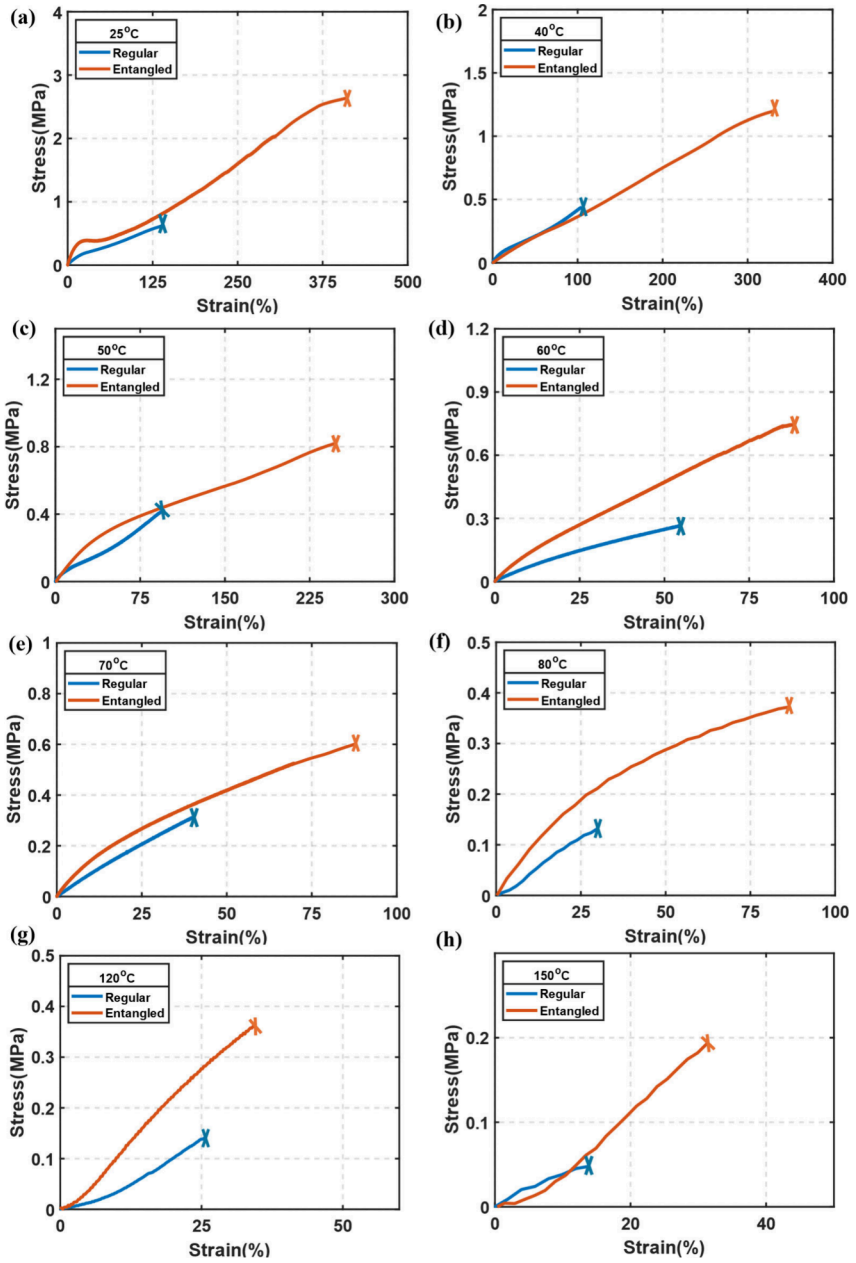

Figure 3. Representative stress−strain curves of Regular and Entangled LCEs, at different temperatures. (a) Comparison at 25 °C. (b) Comparison at 40 °C. (c) Comparison at 50 °C. (d) Comparison at 60 °C. (e) Comparison at 70 °C. (f) Comparison at 80 °C. (g) Comparison at 120 °C. (h) Comparison at 150 °C. The strain rate used was 1%/s.

significantly strengthen LCEs, as shown by the comparison between Entangled and Regular LCEs (Figure 3). At room temperature, Entangled LCEs are not only four times stronger but also three times more stretchable than Regular LCEs, while also exhibiting twice the stiffness even after multiple loading−unloading cycles (Figure S4). This trend was also remarkably consistent across a wide temperature range. LCEs generally exhibit poor mechanical properties at high temperatures due to reduced viscoelastic dissipation mechanisms.[29] While tough at room temperature, they become brittle above their actuation temperature, often leading to unexpected failure.[34] This brittleness poses challenges for practical applications where LCEs must withstand multiple cycles with reliable fracture and fatigue resistance at high temperatures. We found that our Entangled LCEs were stronger and more stretchable compared to Regular LCEs while being stiffer, even at elevated temperatures (Figures 3e−3h). The kneading-induced entanglement strategy presented in this work offers a promising approach to fabricating LCE-based actuators that are both tough and durable under high-temperature conditions.

The effect of kneading begins to saturate after a certain number of cycles, as illustrated in the stress−strain plot (Figure S5), which shows no significant improvement in mechanical properties beyond the sixth cycle of kneading. Therefore, we selected eight cycles as a representative number for this study.

Previous studies investigating the influence of cross-linking density have consistently shown that increasing cross-linking density raises the modulus of LCEs but reduces their failure strain and soft elasticity plateau.[15,22] It is also well established that higher cross-linking density often enhances the strength of

https://doi.org/10.1021/acsami.5c04077
ACS Appl. Mater. Interfaces 2025, 17, 30094−30102

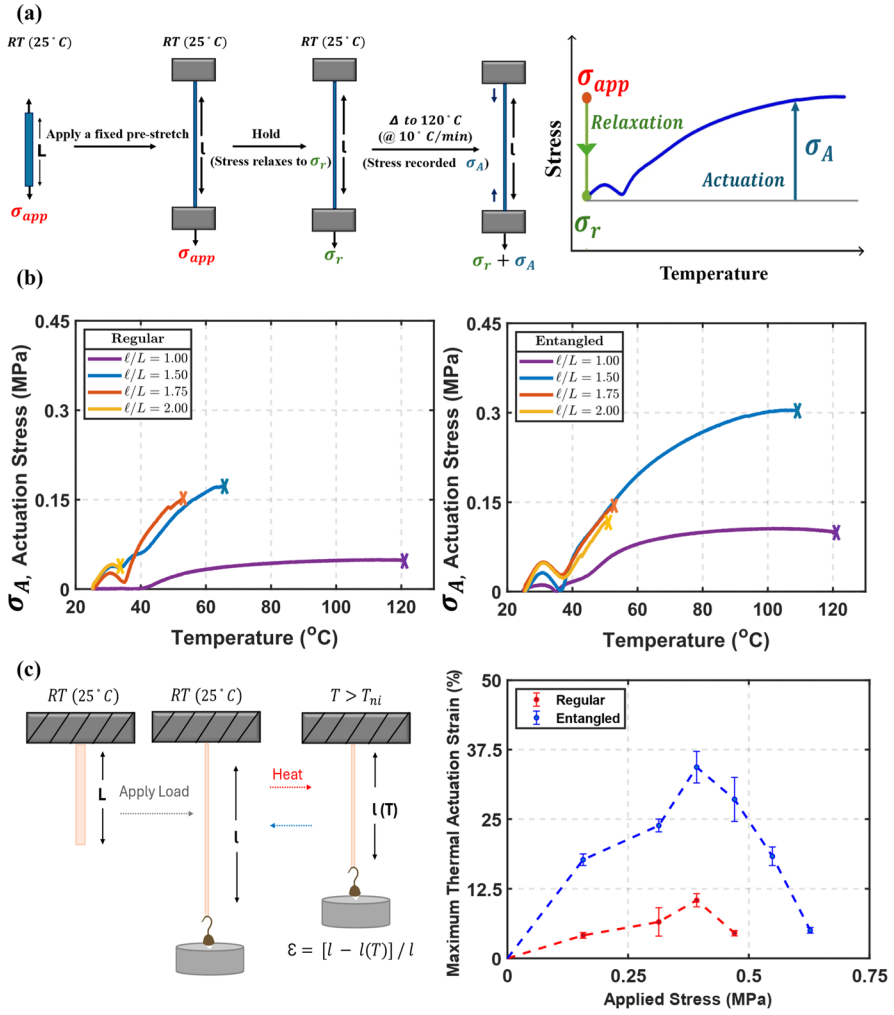

Figure 4. Comparison of actuation performance between Regular and Entangled LCEs. (a) Illustration of actuation stress quantification, where σ_A is defined as the actuation stress. (b) Actuation stress comparison at four different prestretch levels. (c) Actuation strain comparison under various applied loads.

LCEs, as demonstrated experimentally.[15,21,22] In our study, we observed a similar trend where increasing cross-linking made LCEs stronger and stiffer but less stretchable, with a diminished soft elasticity plateau (Figure S6). However, by inducing entanglements in a lower cross-linked LCE network through kneading, we can achieve high stretchability, without compromising strength. This is evidenced by the performance of our Entangled LCE, which exhibited nearly five times higher strain at failure, when compared to its highly cross-linked counterpart with similar strength (Figure S6).

We saw improvement in the mechanical properties of LCEs through entanglements induced through kneading for different cross-linking densities (Figure S7). A higher cross-linking density diminishes the relative effect of chain entanglements.[17] Maintaining a sparsely cross-linked polymer network with long chains allows the benefits of entanglements to be more pronounced, prompting us to adopt a chemical composition with lower cross-linking density for the remainder of the study.

3.3. Thermal-Actuation Behavior of Entangled LCEs. LCEs are well-known for their ability to reversibly transition between ordered (nematic) and disordered (isotropic) states, producing actuation. The temperature at which this phase transition occurs is known as the nematic−isotropic phase transition temperature (T_{ni}). Typically, LCEs respond to temperature changes as the initial order of the mesogen units is gradually disrupted when the material is heated above this temperature.[21,35,36] The temperature dependence of the nematic order is influenced by the physical and chemical properties of the mesogens, as well as the cross-linking density, and can be determined through experimental tests.[13,15] The degree of cross-linking significantly influences the deformation and actuation capabilities of LCEs. Increasing the cross-linking density reduces the deformation capability and the maximum actuation strain. Experimental evidence shows that lowering the cross-linking density allows for greater deformation and improved actuation strain but comes at the cost of reduced stiffness and actuation stress.[13,14]

Our proposed method of fabricating LCEs through kneading to induce entanglements into the network resolves this trade-off between the actuation force and actuation strain. This processing technique increases the actuation force without compromising the actuation strain, offering an optimal balance for actuation performance. We measured the actuation stresses of both Entangled and Regular LCE samples at a fixed length. In the experiments, we first applied a prestretch to a Polydomain LCE sample at 25 °C to align the liquid crystal mesogens. As a result of the prestretch, the length of the sample increased from L to l. We then held the sample in this

https://doi.org/10.1021/acsami.5c04077
ACS Appl. Mater. Interfaces 2025, 17, 30094−30102

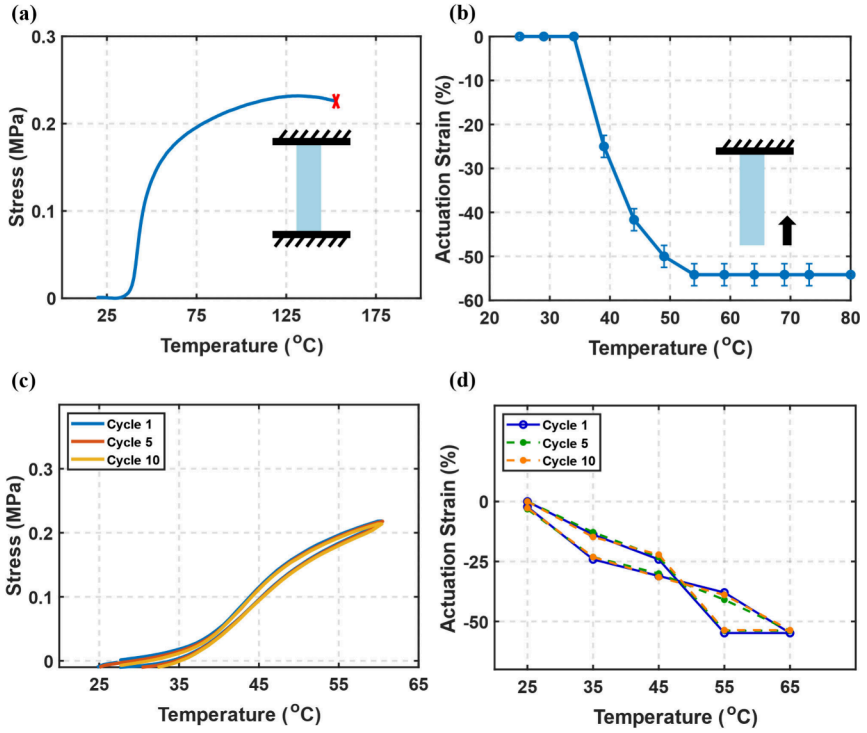

Figure 5. Actuation performance of Entangled Monodomain LCE. (a) High-temperature self-rupture of Entangled Monodomain LCE. (b) Actuation strain of Entangled Monodomain LCE with increasing temperature. (c) Cyclic Actuation Stress of Entangled Monodomain LCE. (d) Cyclic Actuation Strain of Entangled Monodomain LCE.

stretched state for a period of 110 min to allow for stress relaxation, which led to a reduction in stress. The relaxation time was estimated from a stress relaxation test (Figure S8). Subsequently, with the sample length fixed at l, we measured the actuation stress as the temperature increased (Figure 4a). When a stretched LCE sample was heated above its phase transition temperature, a sharp increase in the measured stress value was observed. The actuation stress of both Entangled and Regular LCEs increased with the temperature. The Entangled LCE samples generated larger actuation stresses with rising temperature after relaxation was complete, compared to the Regular LCE samples (Figure 4b). Specifically, the actuation stress of Entangled LCE samples was 1.65, 1.37, and 1.67 times higher than that of Regular LCE samples at l/L = 1.50, 1.75, and 2.00, respectively. In addition, Entangled LCEs demonstrated a higher self-rupture temperature at all prestretch ratios compared to Regular LCEs.

We also performed a similar actuation stress characterization test without any stress-relaxation step and observed the same trend of Entangled LCEs generating higher actuation stresses for all prestretch ratios and having a higher temperature tolerance, compared to Regular LCEs (Figures S9 and S10). Incorporating relaxation time into the actuation stress characterization test was aimed at decoupling the relaxation effects of prestretch from those of thermal actuation, enabling a more accurate understanding of the actuation behavior. We observed consistent actuation stresses in Entangled LCEs over multiple heating−cooling cycles (Figure S11).

To characterize the actuation strain performance of Entangled and Regular LCE samples, we applied a constant load and measured the length change as the ambient temperature increased.

At room temperature (RT = 25 °C), the length of the LCE samples increased from L to l due to the applied weight. After allowing the samples to stabilize for 5 min, the environmental temperature was rapidly raised to T, and the LCE samples exhibited uniaxial contraction, causing their length to decrease from l to $l(T)$. We defined the actuation strain as $\varepsilon = [l - l(T)]/l \times 100\%$. The Entangled LCE samples displayed greater contraction, indicating superior actuation performance and better load carrying capacity across the load spectrum tested (Figure 4c).

It is well understood that cross-linking plays a crucial role in the glass transition, phase transition, and thermal behavior of LCEs. Studies have demonstrated that increasing the cross-linking density raises the glass transition (T_g) and the nematic−isotropic transition (T_{NI}) temperatures, as shown through both theoretical molecular simulations[37] and experimental results.[38] Similarly, we observed that increasing the density of entanglements through kneading produces a comparable effect. Figure S12 shows the differential scanning calorimetry (DSC) measurement comparison between Entangled and Regular LCE samples, revealing that the nematic−isotropic phase transition temperature increases by nearly +4 °C due to the entanglements induced by the kneading process. A highly entangled polymer network increases the required driving force for the phase transition of liquid crystal mesogens. A similar trend was observed near the glass transition temperature (Figure S13), where Entangled LCEs exhibited higher storage and loss moduli compared to Regular LCEs.

3.4. Entanglements as a Pathway for the Fabrication of Monodomain LCEs. Finally, we demonstrated an additional benefit of introducing chain entanglements during LCE synthesis, where entanglements serve as the first cross-

https://doi.org/10.1021/acsami.5c04077
ACS Appl. Mater. Interfaces 2025, 17, 30094−30102

linking step, facilitating the synthesis of Monodomain LCEs. To fabricate Entangled Monodomain LCEs, the kneaded LCE sheet is partially photopolymerized under UV light for a short time. This initial UV cross-linking provides sufficient mechanical integrity to sustain a prestretch in the range of $\lambda = 2-3$, as a fully entangled LCE without any UV cross-linking resembles a highly viscous gel-like state that cannot withstand such deformation. After this step, the LCE is stretched to twice its original length, aligning the mesogens uniaxially. The sample is then fully photopolymerized under UV light to complete the cross-linking reaction, fixing the network in its aligned state (Figure S14).

The Entangled Monodomain LCE can withstand high temperatures without self-rupture, as shown in Figure 5a, inducing approximately 0.3 MPa of actuation stress before rupture at 150 °C. Additionally, the Entangled Monodomain LCE exhibits rapid uniaxial contraction when heated above its phase transition temperature (T_{ni}), with the optimum actuation window observed between 40 and 50 °C (Figures 5b and S15). We did not observe any significant reduction in actuation stress or maximum actuation strain over multiple thermal cycles (Figure 5c and 5d).

This fabrication method is not feasible for Regular LCEs, as the absence of entanglements renders the sample incapable of withstanding even the slight deformation required to align the mesogens. Attempts to uniaxially stretch such samples result in multiple cracks, as shown in Figure S16. This further highlights the benefit of the kneading process to induce entanglements into the polymer network.

4. CONCLUSIONS

In this work, we present a method for inducing a high density of entanglements in liquid crystal polymers through mechanical kneading. The entangled polymer chains are subsequently cross-linked into a polymer network via UV polymerization. The repeated folding and compression cycles in the kneading process result in a network of entanglements, significantly enhancing the strength and stretchability of LCEs for wide ranges of strain rates and temperatures. Additionally, Entangled LCEs exhibited superior actuation performance in a prestretched state, with higher actuation stress and greater contraction compared to Regular LCEs. Finally, we have demonstrated that the chain entanglements alone allow us to prestretch liquid crystal polymers to macroscopically align the mesogens and then cross-link them to synthesize a Monodomain liquid crystal elastomer. Looking ahead, this strategy for inducing entanglements may also be adapted to other morphologies such as fibers or 3D-printed structures. For example, during the kneaded 'dough' stage, the material could be extruded through a syringe to form fiber-like geometries or directly written into complex architectures using direct ink writing, thereby expanding the versatility of LCEs.

ASSOCIATED CONTENT

Supporting Information

The Supporting Information is available free of charge at https://pubs.acs.org/doi/10.1021/acsami.5c04077.

Chemical structures of all chemicals used in LCE synthesis; visual representation of Regular and Entangled LCE; comparison of TGA results between Regular and Entangled LCE; comparison of stress−strain curves between Regular LCE and Entangled LCE after multiple loading−unloading cycles; effect of kneading cycles on LCE; comparison of stress−strain curves between Entangled LCE and Regular LCE (with different cross-linking densities); effect of cross-linking density on entanglements; stress relaxation of Regular and Entangled LCE; detailed actuation stress comparison between Regular and Entangled LCE, with and without stress relaxation; comparison of actuation stress between Regular and Entangled LCE for multiple heating−cooling cycles; effect of entanglements on phase transition behavior of LCE; DMA characterization of Regular and Entangled LCE; illustration of fabrication of Entangled Monodomain LCE; stress−strain curve and phase transition temperature of Entangled Monodomain LCE; failure in fabrication of Regular Monodomain LCE (PDF)

AUTHOR INFORMATION

Corresponding Author

Shengqiang Cai − *Department of Mechanical and Aerospace Engineering and Materials Science and Engineering Program, University of California, San Diego, La Jolla, California 92093, United States;* orcid.org/0000-0002-6852-7680; Email: s3cai@ucsd.edu

Authors

Devyansh Agrawal − *Department of Mechanical and Aerospace Engineering, University of California, San Diego, La Jolla, California 92093, United States*

Gaoweiang Dong − *Materials Science and Engineering Program, University of California, San Diego, La Jolla, California 92093, United States*

Complete contact information is available at: https://pubs.acs.org/10.1021/acsami.5c04077

Notes

The authors declare no competing financial interest.

ACKNOWLEDGMENTS

This work was supported by the U.S. DEVCOM Army Research Office through grant no. W911NF-20-2-0182 and UC San Diego Materials Research Science and Engineering Center (UCSD MRSEC) through grant no. DMR-2011924.

REFERENCES

(1) Ula, S. W.; Traugutt, N. A.; Volpe, R. H.; Patel, R. R.; Yu, K.; Yakacki, C. M. Liquid Crystal Elastomers: An Introduction and Review of Emerging Technologies. *Liq. Cryst. Rev.* **2018**, *6*, 78−107.

(2) Herbert, K. M.; Fowler, H. E.; McCracken, J. M.; Schlafmann, K. R.; Koch, J. A.; White, T. J. Synthesis and Alignment of Liquid Crystalline Elastomers. *Nat. Rev. Mater.* **2022**, *7*, 23−38.

(3) Sun, D.; Zhang, J.; Li, H.; Shi, Z.; Liu, Q.; Chen, S.; Liu, X. Toward Application of Liquid Crystalline Elastomer for Smart Robotics: State of the Art and Challenges. *Polymers* **2021**, *13*, 11.

(4) He, Q.; Wang, Z.; Wang, Y.; Wang, Z.; Li, C.; Cai, S.; et al. Electrospun Liquid Crystal Elastomer Microfiber Actuator. *Sci. Robot.* **2021**, *6*, 57.

(5) Dong, G.; Feng, T.; Chen, R.; Cai, S. Autonomous Thermal Modulator Based on Gold Film-Coated Liquid Crystal Elastomer. *Adv. Mater. Technol.* **2024**, *9*, No. 2400512.

(6) He, Q.; Wang, Z.; Wang, A.; Minori, A.; Tolley, M. T.; Cai, S. Electrically Controlled Liquid Crystal Elastomer-Based Soft Tubular Actuator with Multimodal Actuation. *Sci. Adv.* **2019**, *5*, 10.

(7) Annapooranan, R.; Jeyakumar, S. S.; Chambers, R. J.; Long, R.; Cai, S. Ultra Rate-Dependent Pressure-Sensitive Adhesives Enabled by Soft Elasticity of Liquid Crystal Elastomers. *Adv. Funct. Mater.* **2024**, *34*, 1.
(8) Wang, Y.; He, Q.; Wang, Z.; Zhang, S.; Li, C.; Park, Y.-L.; Cai, S. Liquid Crystal Elastomer Based Dexterous Artificial Motor Unit. *Adv. Mater.* **2023**, *35*, 17.
(9) Wang, Z.; Wang, Y.; Cai, S.; Yang, J. Liquid Crystal Elastomers for Soft Actuators. *Mater. Lab* **2022**, *1*, No. 220030.
(10) Clarke, S. M.; Tajbakhsh, A. R.; Terentjev, E. M.; Remillat, C.; Tomlinson, G. R.; House, J. R. Soft Elasticity and Mechanical Damping in Liquid Crystalline Elastomers. *J. Appl. Phys.* **2001**, *89*, 6530−6535.
(11) Guo, H.; Terentjev, A.; Saed, M. O.; Terentjev, E. M. Momentum Transfer on Impact Damping by Liquid Crystalline Elastomers. *Sci. Rep.* **2023**, *13*, 1.
(12) Annapooranan, R.; Yeerella, R. H.; Chambers, R. J.; Li, C.; Cai, S. Soft Elasticity Enabled Adhesion Enhancement of Liquid Crystal Elastomers on Rough Surfaces. *Proc. Natl. Acad. Sci. U.S.A.* **2024**, *121*, 43.
(13) Brighenti, R.; Cosma, M. P. Smart Actuation of Liquid Crystal Elastomer Elements: Cross-Link Density-Controlled Response. *Smart Mater. Struct.* **2022**, *31*, No. 015012.
(14) Burke, K. A.; Rousseau, I. A.; Mather, P. T. Reversible Actuation in Main-Chain Liquid Crystalline Elastomers with Varying Crosslink Densities. *Polymer* **2014**, *55*, 5897−5907.
(15) Clarke, S. M.; Hotta, A.; Tajbakhsh, A. R.; Terentjev, E. M. Effect of Crosslinker Geometry on Equilibrium Thermal and Mechanical Properties of Nematic Elastomers. *Phys. Rev. E* **2001**, *64*, No. 061702.
(16) Rubinstein, M.; Panyukov, S. Elasticity of Polymer Networks. *Macromolecules* **2002**, *35*, 6670−6686.
(17) Nowak, C.; Escobedo, F. A. Optimizing the Network Topology of Block Copolymer Liquid Crystal Elastomers for Enhanced Extensibility and Toughness. *Phys. Rev. Mater.* **2017**, *1*, No. 035601.
(18) Kong, D.-C.; Yang, M.-H.; Zhang, X.-S.; Fu, Z.-C.; Gao, J.-W. Control of Polymer Properties by Entanglement: A Review. *Macromol. Mater. Eng.* **2021**, *306*, 12.
(19) Nian, G.; Kim, J.; Bao, X.; Suo, Z. Making Highly Elastic and Tough Hydrogels from Doughs. *Adv. Mater.* **2022**, *34*, No. 2206577.
(20) Sun, J.-Y.; Zhao, X.; Illeperuma, W. R. K.; Chaudhuri, O.; Oh, K. H.; Mooney, D. J.; Vlassak, J. J.; Suo, Z. Highly Stretchable and Tough Hydrogels. *Nature* **2012**, *489*, 133−136.
(21) Saed, M. O.; Torbati, A. H.; Starr, C. A.; Visvanathan, R.; Yakacki, C. M. Thiol-Acrylate Main-Chain Liquid-Crystalline Elastomers with Tunable Thermomechanical Properties and Actuation Strain. *J. Polym. Sci., Part B: Polym. Phys.* **2017**, *55*, 157−168.
(22) Saed, M. O.; Torbati, A. H.; Nair, D. P.; Yakacki, C. M. Synthesis of Programmable Main-Chain Liquid-Crystalline Elastomers Using a Two-Stage Thiol-Acrylate Reaction. *J. Vis. Exp.* **2016**, *107*, DOI: 10.3791/53546.
(23) Das, G.; Park, S.-Y. Liquid Crystalline Elastomer Actuators with Dynamic Covalent Bonding: Synthesis, Alignment, Reprogrammability, and Self-Healing. *Curr. Opin. Solid State Mater. Sci.* **2023**, *27*, No. 101076.
(24) Ma, J.; Yang, Z. Smart Liquid Crystal Elastomer Fibers. *Matter* **2025**, *8*, No. 101950.
(25) Wang, Z.; Boechler, N.; Cai, S. Anisotropic Mechanical Behavior of 3D Printed Liquid Crystal Elastomer. *Addit. Manuf.* **2022**, *52*, No. 102678.
(26) Wang, Z.; Wang, Z.; Zheng, Y.; He, Q.; Wang, Y.; Cai, S. Three-Dimensional Printing of Functionally Graded Liquid Crystal Elastomer. *Sci. Adv.* **2020**, *6*, 39.
(27) Norioka, C.; Inamoto, Y.; Akifumi, H.; Kawamura, C.; Miyata, T. A Universal Method to Easily Design Tough and Stretchable Hydrogels. *NPG Asia Mater.* **2021**, *13*, 1.
(28) Kim, J.; Zhang, G.; Shi, M.; Suo, Z. Fracture, Fatigue, and Friction of Polymers in Which Entanglements Greatly Outnumber Cross-Links. *Science* **2021**, *374*, 212−216.
(29) Annapooranan, R.; Wang, Y.; Cai, S. Highly Durable and Tough Liquid Crystal Elastomers. *ACS Appl. Mater. Interfaces* **2022**, *14*, 2006−2014.
(30) Zou, W.; Lin, X.; Terentjev, E. M. Amine-Acrylate Liquid Single Crystal Elastomers Reinforced by Hydrogen Bonding. *Adv. Mater.* **2021**, *33*, 30.
(31) Dong, G.; Zhao, F.; Gao, Z.; Cai, S. Liquid Crystal Elastomer for Compression Therapy. *Adv. Healthcare Mater.* **2025**, *14*, 3.
(32) Lin, X.; Zou, W.; Terentjev, E. M. Double Networks of Liquid-Crystalline Elastomers with Enhanced Mechanical Strength. *Macromolecules* **2022**, *55*, No. 2402881.
(33) Zhang, S.; Wang, Z.; Zhang, J.; Liu, J.; Qin, S.; Ren, Y.; Zhang, L.; Yang, W. Healable and Multi-Driving Mode Soft Actuator Enabled by Disulfide-Bonded Liquid Crystal Elastomers. *Chem. Eng. J.* **2024**, *491*, 152.
(34) Annapooranan, R.; Cai, S. Thermally Induced Self-Rupture of a Constrained Liquid Crystal Elastomer. *Eng. Fract. Mech.* **2022**, *269*, No. 108584.
(35) Yakacki, C. M.; Saed, M.; Nair, D. P.; Gong, T.; Reed, S. M.; Bowman, C. N. Tailorable and Programmable Liquid-Crystalline Elastomers Using a Two-Stage Thiol−Acrylate Reaction. *RSC Adv.* **2015**, *5*, 18997−19001.
(36) Li, Y.; Liu, T.; Rios, V.; Xia, O.; He, M.; Yang, W. Liquid Crystalline Elastomers Based on Click Chemistry. *ACS Appl. Mater. Interfaces* **2022**, *14*, 14842−14858.
(37) Li, Z.; Liu, Y. The Effect of Crosslinking Rate on the Thermal and Mechanical Properties of Liquid Crystal Elastomers: A Molecular Dynamics Study. *Mater. Today Commun.* **2024**, *40*, No. 110201.
(38) Ware, T. H.; Perry, Z. P.; Middleton, C. M.; Iacono, S. T.; White, T. J. Programmable Liquid Crystal Elastomers Prepared by Thiol-Ene Photopolymerization. *ACS Macro Lett.* **2015**, *4*, 942−946.

https://doi.org/10.1021/acsami.5c04077
ACS Appl. Mater. Interfaces 2025, 17, 30094−30102